

Decentralized Motion Control of Mobile Manipulator

Tan Tung Phan, Jin-Ho Suh and Sang Bong Kim.

Department of Mechanical Engineering, Pukyong National University, Busan, Korea
(Tel +82-51-620-1606, E-mail: phtantung@yahoo.com)

Abstract: The mobile platform-manipulator discussed in this paper is a three link manipulator mounted on a mobile platform. This mobile manipulator is used for welding operation and it is able to operate in a narrow space. The task of the torch, which is mounted at the end effector of the manipulator, is to track along the seam line and the task of the mobile platform is to move the origin point of the manipulator in order to go away from the singularity of the manipulator's configuration. In this paper, the path planning for the motion of two subsystems (i.e., the manipulator and the mobile platform) was presented by the decentralized control method. Two controllers for the mobile platform and the manipulator were designed, and the relationship between the independent controllers is its state information. The simulation results are also presented to demonstrate the effectiveness of the control method.

Keywords: decentralized motion control, platform, manipulator, welding path reference.

1. INTRODUCTION

The mobile platform manipulator is a topic that has been studied by many researchers in recent years. Its advantages are the large operation space and it can perform many requirements of different tasks.

The kinematic model for the mobile platform was presented in [8], [9], [10], for the mobile manipulator platform in [2], [3], [4], [6], and the decentralized control also discussed in [5], [9]. Decentralized motion control for the mobile manipulator is a interesting problem that is still studying. The manipulator presented in this paper is the planar three-link manipulator, it has three links and three revolute joints. This manipulator is mounted at the center point of a two-wheeled mobile platform.

In this paper, we assume that the mobile platform and the manipulator move on low speed because the welding velocity is just about 7.5mm/s, so we skip the inertia and the slipping between the wheels and the floor. This mobile manipulator is used to weld the planed smooth welding lines. In [7], the authors used a two-wheeled robot with the sliding-torch, we are using the mobile manipulator with the torch is mounted on the end effector of the manipulator, so it can weld in even small space if the mobile robot can not move into it.

The requirements of welding task are that the end effector must track along the seam with a constant velocity and the torch must incline to the seam with a constant angle. Using the decentralized motion control, we can easy control two subsystems, so that the complicity of model will reduce when to compare the centralized motion control. The relationship between two subsystems is given by its state information.

We propose the designed controllers based on the Lyapunov control function to enhance the tracking properties of the mobile manipulator.

2 KINEMATIC EQUATIONS

2.1 Kinematic equations of the manipulator

We consider a three-link manipulator as in Fig. 1. We attach a Cartesian coordinate frame (frame 1) at the joint 1 of the manipulator. Because this frame is fixed at the center of the mobile platform, so this frame is called the local frame

Let us denote:

l_1, l_2, l_3 : the length of the links.

J_1, J_2, J_3 : the symbols of the revolute joints.

$\theta_1, \theta_2, \theta_3$: the angles of the joints.

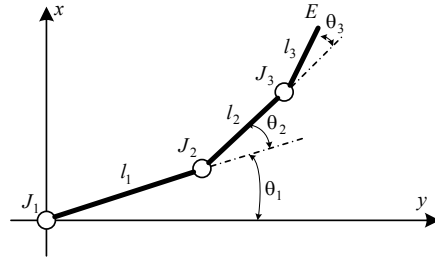


Fig 1 : The planar three-link manipulator in frame 1

From [1] we get:

$$\begin{bmatrix} \theta_1 \\ \theta_2 \\ \theta_3 \end{bmatrix} = J^{-1} \begin{bmatrix} {}^1P_{Ex} \\ {}^1P_{Ey} \\ {}^1\phi_{Ez} \end{bmatrix} \quad (1)$$

where J is the Jacobian matrix.

$$J = \begin{bmatrix} -l_3S_{123} - l_2S_{12} - l_1S_1 & -l_3S_{123} - l_2S_{12} & -l_3S_{123} \\ l_3C_{123} + l_2C_{12} + l_1C_1 & l_3C_{123} + l_2C_{12} & l_3C_{123} \\ 1 & 1 & 1 \end{bmatrix}$$

$$S_1 = \sin(\theta_1); \quad S_{12} = \sin(\theta_1 + \theta_2); \quad S_{123} = \sin(\theta_1 + \theta_2 + \theta_3);$$

$$C_1 = \cos(\theta_1); \quad C_{12} = \cos(\theta_1 + \theta_2); \quad C_{123} = \cos(\theta_1 + \theta_2 + \theta_3);$$

$\theta = [\theta_1 \ \theta_2 \ \theta_3]^T$: the joint variable vector of the manipulator.

${}^1P_E = [{}^1P_{Ex} \ {}^1P_{Ey} \ {}^1\phi_E]^T$: the position vector of the end effector with respect to the local frame .

The values of $\theta_1, \theta_2, \theta_3$ are determined as the following:

$$\theta_2 = \text{acos} \left(\frac{{}^1P_{Ex}^2 + {}^1P_{Ey}^2 - l_1^2 - l_2^2}{2l_1l_2} \right). \quad (2)$$

$$\theta_1 = \text{atan2}({}^1P_{Ex}, {}^1P_{Ey}) - \text{atan2}(l_2S_2, l_1 + l_2C_2) \quad (3)$$

$$\theta_3 = \Psi - \theta_1 - \theta_2 \quad (4)$$

where Ψ is the angle from the torch to the seam, and this angle is depended on the welding condition.

When the end effector of the manipulator moves a small distance, the kinematic equation (1) becomes:

$$\begin{aligned} \begin{bmatrix} d\theta_1 \\ d\theta_2 \\ d\theta_3 \end{bmatrix} &= J^{-1} \begin{bmatrix} {}^1 dp_{Ex} \\ {}^1 dp_{Ey} \\ {}^1 d\phi_E \end{bmatrix} \Rightarrow \begin{bmatrix} d\theta_1 \\ d\theta_2 \\ d\theta_3 \end{bmatrix} = J^{-1} \begin{bmatrix} {}^1 \dot{p}_{Ex} \\ {}^1 \dot{p}_{Ey} \\ {}^1 \dot{\phi}_E \end{bmatrix} \\ &\Rightarrow \begin{bmatrix} \dot{\theta}_1 \\ \dot{\theta}_2 \\ \dot{\theta}_3 \end{bmatrix} = J^{-1} \begin{bmatrix} {}^1 v_{Ex} \\ {}^1 v_{Ey} \\ {}^1 \omega_E \end{bmatrix} \end{aligned} \quad (5)$$

where $d\theta = [\dot{\theta}_1 \ \dot{\theta}_2 \ \dot{\theta}_3]^T$ is the angular velocity vector of the joints, $dp_E = [{}^1 v_{Ex} \ {}^1 v_{Ey} \ {}^1 \omega_E]^T$ is the velocity vector of the end effector with respect to the frame 1.

2.2 Kinematics equation of the mobile platform

We consider a two-wheeled mobile platform in Fig. 2. When the mobile platform is moving in the horizontal plane, the translational velocity of the mobile platform is v_p , and the angular velocity is ω_p . The relationship between v_p , ω_p and the angular velocities of the two driving wheels is:

$$\begin{bmatrix} \omega_{rW} \\ \omega_{lW} \end{bmatrix} = \begin{bmatrix} 1/r & b/r \\ 1/r & -b/r \end{bmatrix} \begin{bmatrix} v_p \\ \omega_p \end{bmatrix} \quad (6)$$

where ω_{rW}, ω_{lW} are the angular velocities of the right and left wheel, b is the distance from the mobile platform's center to the driving wheel, and r is the radius of the wheel.

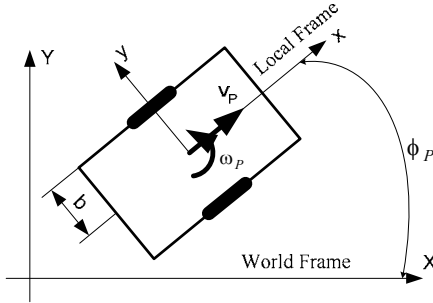


Fig 2 : Scheme for deriving the kinematic equations of the two-wheeled platform

3. CONTROLLERS DESIGN

We assume that the wheels roll and avoid slipping. The relation of the coordinates of the mobile manipulator with the reference welding path is shown in Fig. 3.

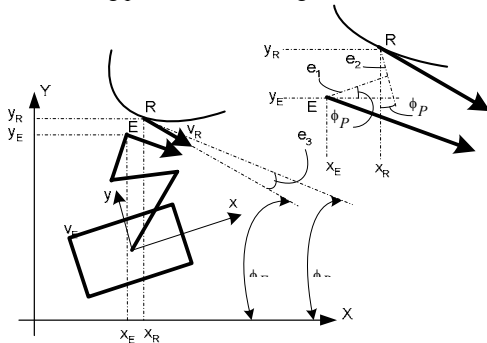


Fig3 Scheme for deriving the kinematic equations.

A reference point R, which has the coordinates (x_R, y_R) and the heading angle ϕ_R , is moving with the constant velocity v_r on the reference welding paths must satisfy the equations:

$$\dot{x}_R = v_R \cos(\phi_R), \quad (7.a)$$

$$\dot{y}_R = v_R \sin(\phi_R), \quad (7.b)$$

$$\dot{\phi}_R = \omega_R. \quad (7.c)$$

Our objective is to design controllers so that the end effector, which has the coordinates (x_E, y_E) and the heading angle ϕ_E , tracks to the reference point R. We define the tracking errors $e = [e_1 \ e_2 \ e_3]^T$, as shown in Fig. 3, as:

$$\begin{bmatrix} e_1 \\ e_2 \\ e_3 \end{bmatrix} = \begin{bmatrix} \cos(\phi_E) & \sin(\phi_E) & 0 \\ -\sin(\phi_E) & \cos(\phi_E) & 0 \\ 0 & 0 & 1 \end{bmatrix} \begin{bmatrix} x_R - x_E \\ y_R - y_E \\ \phi_R - \phi_E \end{bmatrix} \quad (8)$$

We will design a controllers to archive $e_i \rightarrow 0$ when $t \rightarrow \infty$, and hence the end effector tracks to its reference point R. We can get Eq. (9) from the derivative of Eq. (8):

$$\begin{aligned} \begin{bmatrix} \dot{e}_1 \\ \dot{e}_2 \\ \dot{e}_3 \end{bmatrix} &= \omega_E \begin{bmatrix} -\sin(\phi_E) & \cos(\phi_E) & 0 \\ -\cos(\phi_E) & -\sin(\phi_E) & 0 \\ 0 & 0 & 0 \end{bmatrix} \begin{bmatrix} x_R - x_E \\ y_R - y_E \\ \phi_R - \phi_E \end{bmatrix} + \\ &+ \begin{bmatrix} \cos(\phi_E) & \sin(\phi_E) & 0 \\ -\sin(\phi_E) & \cos(\phi_E) & 0 \\ 0 & 0 & 1 \end{bmatrix} \begin{bmatrix} \dot{x}_R - \dot{x}_E \\ \dot{y}_R - \dot{y}_E \\ \dot{\phi}_R - \dot{\phi}_E \end{bmatrix} \end{aligned} \quad (9)$$

The Lyapunov function is chosen as Eq.(10) and its derivative is given by Eq.(11):

$$\dot{V}_0 = \frac{1}{2} \dot{e}_1^2 + \frac{1}{2} \dot{e}_2^2 + \frac{1}{2} \dot{e}_3^2 \geq 0 \quad (10)$$

$$\Rightarrow \dot{V}_0 = \dot{e}_1 e_1 + \dot{e}_2 e_2 + \dot{e}_3 e_3 \quad (11)$$

From Eqs (8),(9),(11) we get

$$\begin{aligned} \dot{V}_0 &= \begin{bmatrix} e_1 \cos(\phi_E) & e_1 \sin(\phi_E) & 0 \\ -e_2 \sin(\phi_E) & e_2 \cos(\phi_E) & 0 \\ 0 & 0 & 1 \end{bmatrix} \begin{bmatrix} \dot{x}_R - \dot{x}_E \\ \dot{y}_R - \dot{y}_E \\ \dot{\phi}_R - \dot{\phi}_E \end{bmatrix} \\ &= \begin{bmatrix} e_1 \cos(\phi_E) & e_1 \sin(\phi_E) & 0 \\ -e_2 \sin(\phi_E) & e_2 \cos(\phi_E) & 0 \\ 0 & 0 & 1 \end{bmatrix} \begin{bmatrix} v_R \cos(\phi_R) - v_E \cos(\phi_E) \\ v_R \sin(\phi_R) - v_E \sin(\phi_E) \\ \omega_R - \omega_E \end{bmatrix} \\ &\Rightarrow \dot{V}_0 = (v_R \cos(e_3) - v_E) e_1 + \left(v_R e_2 e_3 \frac{\sin(e_3)}{e_3} + \omega_R - \omega_E \right) e_3. \end{aligned} \quad (12)$$

In order to satisfy its stability, we must choose the values of v_E and ω_E , so that the Eq. (12) archives the negative value. We can choose as follows;

$$v_E = v_R \cos(e_3) + k_1 e_1. \quad (13)$$

$$\omega_E = v_R e_2 \frac{\sin(e_3)}{e_3} + \omega_R + k_3 e_3. \quad (14)$$

where k_1, k_3 are positive values.

3.1 Design controller for the manipulator

For Body motion in a plane, the absolute velocity vector of a point E (i.e. the end effector) includes the absolute velocity vector of point P (i.e. the center point of mobile platform), plus to the relative velocity vector of point E with respect to point P. The absolute velocity vector of point P includes two components: the translational velocity and the rotational velocity. Scheme to calculate the velocities of the plane motion of points E and P is illustrated in Fig.4.

We get the equation as follows:

$$v_E = v_P + \omega_P \times P_E + v_{E/P} \quad (15)$$

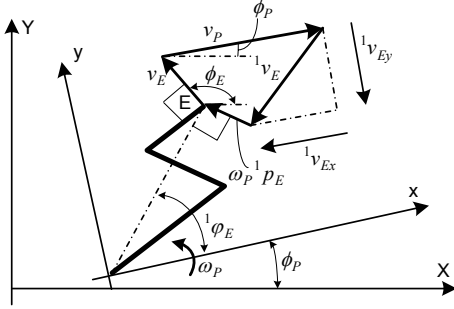


Fig4 Scheme to calculate the velocities.

Eq (15) can be rewritten to become the system equation (16)

$${}^1v_{Ex} = v_E \cos(\phi_E - \phi_P) + \omega_P {}^1P_E \sin(\phi_E) - v_P, \quad (16.a)$$

$${}^1v_{Ey} = v_E \sin(\phi_E - \phi_P) + \omega_P {}^1P_E \cos(\phi_E), \quad (16.b)$$

$${}^1\omega_E = \omega_E - \omega_P \quad (16.c)$$

or, in matrix form:

$$\begin{bmatrix} {}^1v_{Ex} \\ {}^1v_{Ey} \\ {}^1\omega_E \end{bmatrix} = \begin{bmatrix} -1 & {}^1P_{Ey} \\ 0 & -{}^1P_{Ex} \\ 0 & -1 \end{bmatrix} \begin{bmatrix} v_P \\ \omega_P \end{bmatrix} - \begin{bmatrix} \cos(\phi_E - \phi_P) & 0 \\ \sin(\phi_E - \phi_P) & 0 \\ 0 & 1 \end{bmatrix} \begin{bmatrix} v_E \\ \omega_E \end{bmatrix} \quad (17)$$

From Eqs. (5), (16), we derive the angular velocities of the revolute joints.

$$\begin{bmatrix} d\theta_1 \\ d\theta_2 \\ d\theta_3 \end{bmatrix} = J^{-1} \begin{bmatrix} {}^1v_{Ex} \\ {}^1v_{Ey} \\ {}^1\omega_E \end{bmatrix} \quad (18)$$

This equation is control law for the manipulator. From Eq (18) we can find that the inputs of the controller are the errors from the sensors (i.e. vector $[v_E \ \omega_E]^T$), the joint variables (i.e. vector $\theta = [\theta_1 \ \theta_2 \ \theta_3]^T$), and the velocity vector of the center point of the mobile platform $[v_P \ \omega_P]^T$. The outputs are the angular velocities of the joints.

3.2 Design controller for the platform

In this section, we will consider two cases such that the mobile platform moves along a defined trajectory, and it moves to satisfy the condition that is the singularity is not occurred.

*** Case 1: the mobile platform's trajectory is known in advance**

We can choose a trajectory for the mobile platform with a condition that the singularity is not occurred for the manipulator, so that the mobile platform actions can be planed off-line. This case is used for a simple reference welding path, so we can imagine and check the singularity condition by visual.

For example, with the reference welding path in Fig. 7, we can choose the control law for the mobile platform as in Table 1.

Table 1 Control law for the mobile platform.

Time (s)	v_p (mm/s)	ω_p (rad/s)
0~20	6.59	0
20~60	19.73	0.0393
60~120	0	-0.0262
120~140	4.13	0

The mobile platform's trajectory is shown in Fig. 8. We can choose any control law for the mobile platform's controller if the singularity for the manipulator is not occurred. This is a characteristic of the decentralized control and this controller can not receive any environment information.

*** Case 2: the mobile platform's trajectory satisfies non-singularity condition**

We find that, Eq. (18) can be solved if the determinant of matrix J is not going to zero. This means that the angle value of the joint 2 (i.e. θ_2 angle) must not equal to 0 or π . If θ_2 equal to 0 or π , the manipulator's singularity will occur. The mobile platform's path planning for this case is how to get the suitable translational and angular velocities to satisfy the non-singularity condition.

From above, we find that we can study a two link manipulator instead of the three-link manipulator, and the two link manipulator is shown in Fig. 5. The point J_3 is moving with the velocity v_{J_3} , and the distance R changes with respect to time. In order to avoid the singularity, the point P must move to the relative velocity v_{Comp} with respect to the point J_3 , the value of v_{Comp} is chosen through experiments. The mobile platform's velocity v_P determined by Eq. (21)..

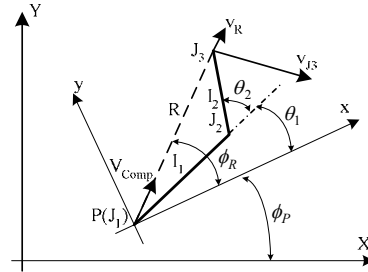


Fig5 Scheme for deriving the mobile platform's controller.

From Fig.5 we get:

$$R = \sqrt{l_1^2 + l_2^2 + 2l_1l_2 \cdot \cos(\theta_2)}. \quad (19)$$

$$\Rightarrow v_R = \dot{R} = \frac{-l_1l_2 \sin(\theta_2) \dot{\theta}_2}{R} \quad (20)$$

$$\phi_R = \text{atan2}({}^1P_{J_3y}, {}^1P_{J_3x}). \quad (21)$$

$${}^1P_{J_3x} = l_1 \cos(\theta_1) + l_2 \cos(\theta_1 + \theta_2) \quad (22.a)$$

$${}^1P_{J_3y} = l_1 \sin(\theta_1) + l_2 \sin(\theta_1 + \theta_2) \quad (22.b)$$

In order to get safety, we limit the operation angle of the joint 2 from θ_{Saf} to $\pi - \theta_{Saf}$. To avoid the singularity, point P must move with a velocity v_P when $\theta_2 < \theta_{Saf}$ or $\theta_2 > \pi - \theta_{Saf}$.

$$v_P = v_R \pm v_{Comp} + v_{J_3} \quad (23)$$

where the sign + when $\theta_2 < \frac{\pi}{2}$, and the sign - when $\theta_2 > \frac{\pi}{2}$

or, in matrix form:

$$\begin{bmatrix} v_{Px} \\ v_{Py} \end{bmatrix} = \begin{bmatrix} v_{Rx} \\ v_{Ry} \end{bmatrix} \pm \begin{bmatrix} v_{Comp_x} \\ v_{Comp_y} \end{bmatrix} + \begin{bmatrix} v_{J_3x} \\ v_{J_3y} \end{bmatrix}, \quad (24.a)$$

$$\omega_P = {}^1\dot{\phi}_P. \quad (24.b)$$

where ${}^1\phi_P = \text{atan2}(v_{Py}, v_{Px})$.

The velocity of point J₃ is determined as follows:

$$\begin{bmatrix} v_{J_3x} \\ v_{J_3y} \\ \omega_{J_3} \end{bmatrix} = \begin{bmatrix} -l_1 S_1 - l_2 S_{12} & -l_2 S_{12} & 0 \\ l_1 C_1 + l_2 C_{12} & l_2 C_{12} & 0 \\ 0 & 0 & 1 \end{bmatrix} \begin{bmatrix} d\theta_1 \\ d\theta_2 \\ d\theta_1 + d\theta_2 \end{bmatrix} \quad (25)$$

Eqs. (24) is control law of the mobile platform, and the inputs of this controller are the angle values and the angular velocity of the joints. The outputs are the angular velocities of two wheels, which are determined from Eq. (6).

4. MEASUREMENT OF THE ERRORS

We use again the measured method in [7] to detect the errors. The sensor includes two rollers and two potentiometers as shown in Fig. 6.

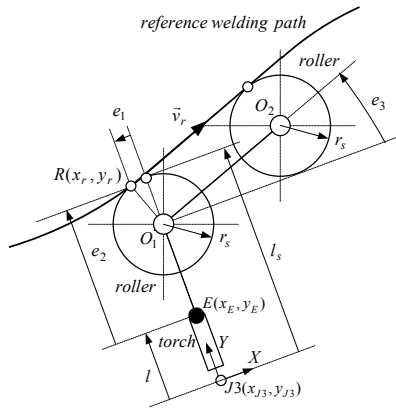


Fig.6 Scheme for measuring the errors.

Two rollers are placed in points O_1 and O_2 , the roller's radius are r_s , and the length from the center of joint 3 to the quarter point on the roller 1 is l_s . We have two potentiometers: one is assembled at O_1 to measure the angle error e_3 , one is assembled along the line O_1J_3 to measure the straight errors e_1, e_2 . We have the relationships as follows:

$$e_1 = -r_s \sin(e_3) \quad (26.a)$$

$$e_2 = (l_s - l) - r_s (l - \cos(e_3)) \quad (26.b)$$

$$e_3 = \angle(O_1J_3 \ O_1O_2) - \frac{\pi}{2} \quad (26.c)$$

5. RESULTS OF SIMULATION AND DISCUSSIONS

5.1 Results of simulation in Case 1

To verify the effectiveness of the proposed method and controllers, simulations have been done for the mobile manipulator with a defined reference welding path, which is similar to the proposed path in [7]. The numerical values used in this simulation are given in Table 2.

Table 2 The numerical values and initial values for simulation.

Parameters	Values	Units
l_1	0.250	M
l_2	0.150	M
l_3	0.070	M
b	0.105	M
r_s	0.025	M
x_R	0.280	M
y_R	0.040	M
ϕ_R	0	deg.
x_E	0.275	M
y_E	0.395	M
ϕ_E	15	deg.
v_R	0.0075	m/s
θ_1 (at beginning)	55.58	deg.
θ_2 (at beginning)	111.57	deg.
θ_3 (at beginning)	-62.45	deg.
k_1	4.8	
k_2	0.521	

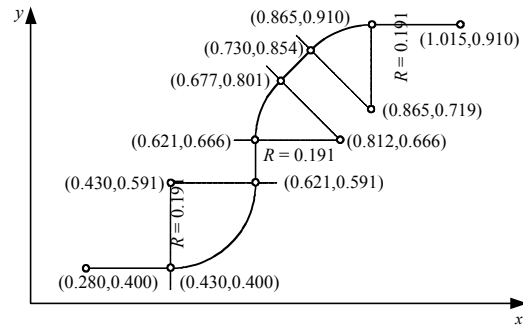


Fig.7 Reference welding path.

This simulation was done for a mobile manipulator where the mobile platform's control law is given in Table 1, section 3.2. The manipulator's control law in Eq.(18) is used. The simulation results are given in Fig. 8-15. With this simulation values, the errors go to nearly zero after about 8 second. But the convergence of the point E toward the point R is rather fast, and after 2 second the distance between two points is 1.2 mm, after 4 second is 0.4 mm with the initial declination of 5mm.

With the simulation results, we can find that the torch tracks nearly the welding point after 4-5 sec, and the control law of the mobile platform can predefine with the non singularity condition.

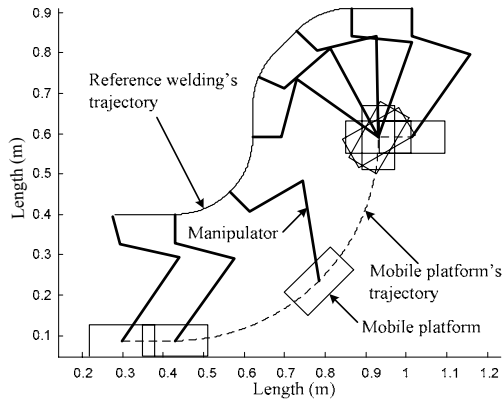


Fig. 8 The mobile manipulator is tracking along the welding path (in case 1 with the mobile platform trajectory in advance)

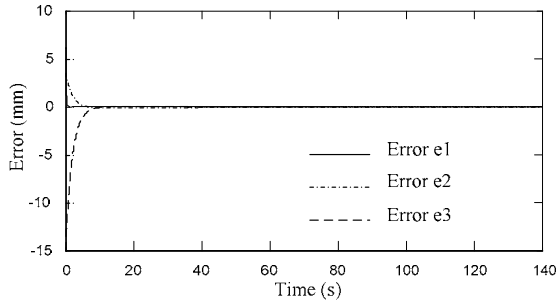


Fig. 9 The tracking errors e_1 , e_2 , e_3

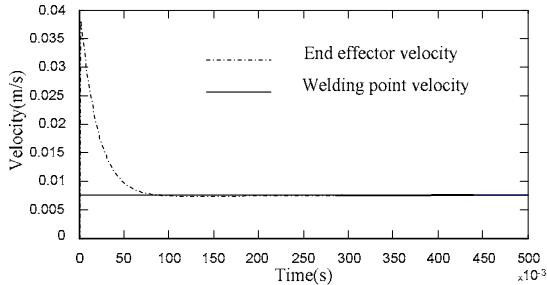


Fig. 10 The velocities of the welding point and the end effector (the torch) in the first 5 seconds.

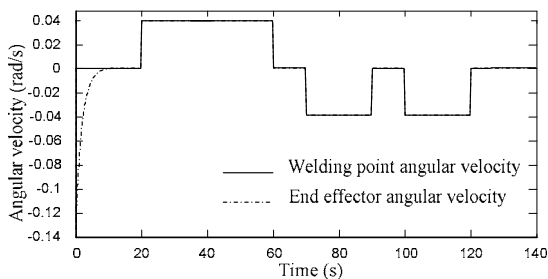


Fig. 11 The angular velocities of the welding point and the end effector

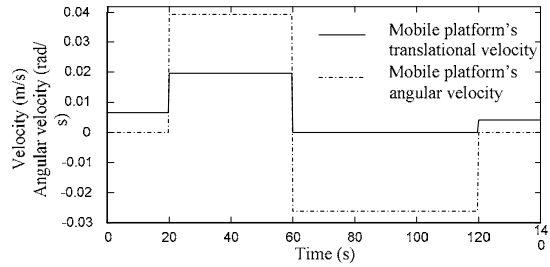


Fig. 12 The translational velocity and the angular velocity of the mobile platform's center point.

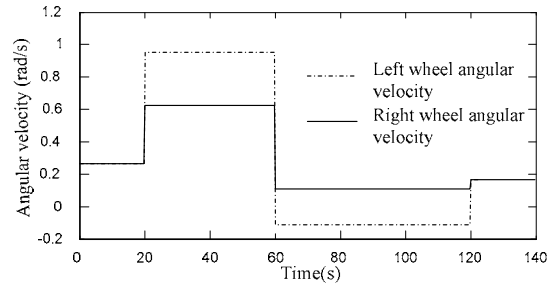


Fig. 13 The angular velocities of two wheels of the platform.

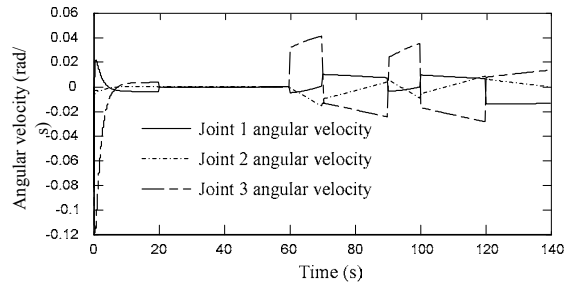


Fig. 14 The angular velocities of three revolute joints of the manipulator.

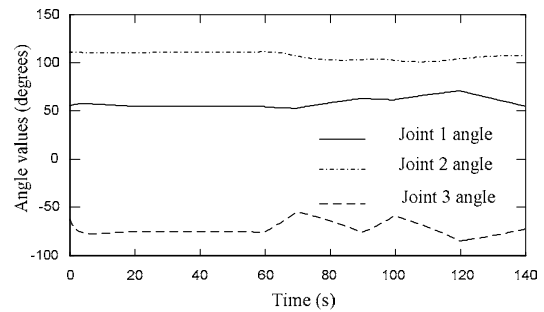


Fig. 15 The angle values of three revolute joints.

5.2 Results of simulation in Case 2

Fig.16 ~ 20 are the simulation results for the case 2, and the reference welding trajectory is also similar in the case 1. The mobile manipulator's parameters are not changing and also the initial conditions are not changing. The mobile platform's controller is Eq (24), the v_{Comp} is chosen as follows:

$$v_{Comp} = 0.005 \text{ m/s} \quad \text{when} \quad \frac{\pi}{6} < \theta_2 < \frac{5\pi}{6}$$

$$v_{Comp} = 0.01 \text{ m/s} \quad \text{when} \quad \frac{5\pi}{6} < \theta_2 < \frac{\pi}{6}$$

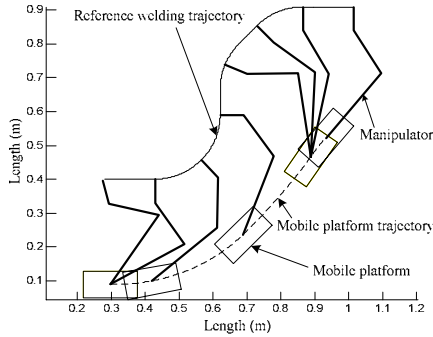


Fig. 16 The mobile manipulator is tracking along the welding path (Case 2 with the mobile platform from away the singularity)

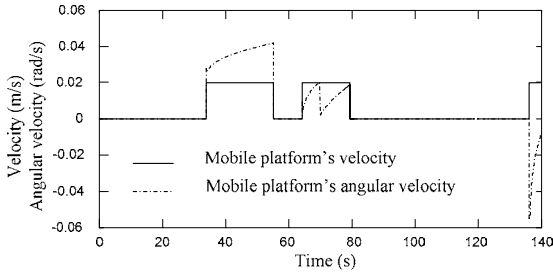


Fig. 17 The translational velocity and the angular velocity of the mobile platform's center point.

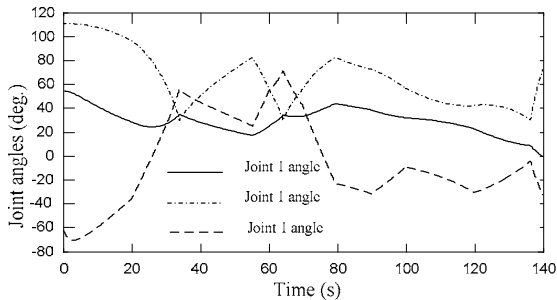


Fig. 18 The angle values of three revolute joints of the manipulator.

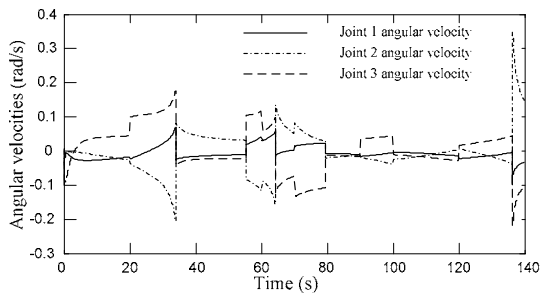


Fig. 19 The angular velocities of three revolute joints of the manipulator.

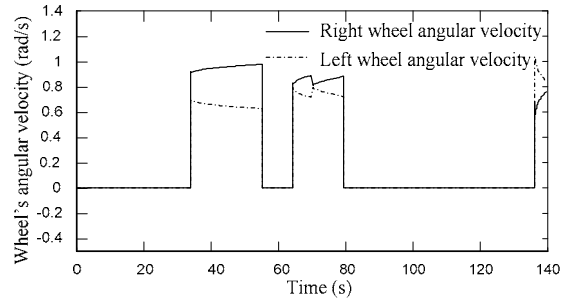


Fig. 20 The angular velocities of two wheels of the platform.

6. CONCLUSIONS

A decentralized control method based on the Lyapunov control function was proposed. The simulation results are shown that the controllers can be used for the mobile manipulators. Because of the independent of the mobile platform's controller from the tracking, so we can design the mobile platform's controller to avoid the obstacles in the future. This will be simple than one centralized controller for the platform plus the manipulator.

REFERENCES

- [1] Ph. J. McKerrow, *Introduction to Robotics*, Addison-Wesley Publishers, 1991.
- [2] Homayoun Seraji "Configuration control of rover-mounted manipulators" *Proc. of the IEEE International Conference on Robotics and Automation*, Vol.3, pp. 2261-2266, 1995.
- [3] B. Bayle, I. Y. Fourquet, F. Lamiroux, M. Renaud "Kinematic Control of Wheeled Mobile Manipulators" *Proc. of the IEEE/RSJ Int. Conf. on Intelligent Robots and Systems*, Vol. 2, pp 1572-1577, 2002..
- [4] W. S. Yoo, J. D. Kim, S. J. Na "A study on a mobile platform-manipulator welding system for horizontal fillet joints" *Mechatronics* Vol 11, pp 853-868, 2001.
- [5] Michel Abou-Samah, Venkat Krovi "Decentralized Kinematic Control of a Cooperating System of Mobile Manipulators" *Proc. of IMECE'02*, Louisiana, 2002..
- [6] Gilles Foulon, J. Yves Fourquet, Marc Renaud "Planning Point to Point Paths for Non-holonomic Mobile Manipulators" *Proc. of the IEEE/RSJ. International Conference on Intelligent Robots and Systems*, pp 374-379, 1998..
- [7] Tr. H. Bui, T. T. Nguyen, T. L. Chung, Sang Bong Kim "A Simple Nonlinear Control of a Two-Wheeled Welding Mobile Robot" *Trans. on Control Automation, and Systems Engineering*, Vol.4, No. 4, pp. 318-324, 2002
- [8] Yutaka Kanayama "Two Dimensional Wheeled Vehicle Kinematic", *Proc. of the IEEE International Conference*, Vol. 4, pp 3079-3084, 1994.
- [9] Thomas Burke, Hugh F. Durrant-Whyte "Kinematic for Modular Wheeled Mobile Robots" *Proc. of the IEEE/RSJ International Conference on Intelligent Robots and Systems*, pp 1279-1286, 1993..
- [10] Takatori Fukao, Hiroshi Nakagawa, and Norihiko Adachi "Adaptive Tracking Control of a Nonholonomic Mobile Robot" *Trans. on Robotics and Automation*, Vol. 16, No. 5, pp. 609-615, 2000.
- [11] John Lloyd and Vincent Hayward "Singularity Control of Robot manipulator using Closed form Kinematic Solutions" *Conference on Electrical and Computer Engineering*, Vol.2, pp. 1065~1068, 1993.